NASA TECHNICAL NOTE

NASA TN D-5952

A METHOD FOR PREDICTING PRESSURES ON ELLIPTIC CONES AT SUPERSONIC SPEEDS

by George E. Kaattari

Ames Research Center

Moffett Field, Calif. 94035

NATIONAL AERONAUTICS AND SPACE ADMINISTRATION • WASHINGTON, D. C. • AUGUST 1970

1. Report No.	2. Government Accession No.	3. Recipient's Catalog No.
NASA TN D-5952		

4. Title and Subtitle	5. Report Date
A METHOD FOR PREDICTING PRESSURES ON ELLIPTIC CONES AT SUPERSONIC SPEEDS	August 1970
	6. Performing Organization Code
7. Author(s)	8. Performing Organization Report No.
George E. Kaattari	A-3642
	10. Work Unit No. 124-64-05-01-00-21
9. Performing Organization Name and Address	11. Contract or Grant No.
NASA Ames Research Center Moffett Field, Calif., 94035	
	13. Type of Report and Period Covered
12. Sponsoring Agency Name and Address	Technical Note
National Aeronautics and Space Administration Washington, D.C. 20546	14. Sponsoring Agency Code

15. Supplementary Notes

16. Abstract

A method is presented for estimating the pressure distribution over elliptic cones at supersonic Mach numbers and angle of attack. The method is based on an empirical correlation between experimental pressures in the symmetry planes of elliptic cones and the pressures given by two-dimensional shock theory. The method is applicable for Mach numbers greater than 2, for cones whose ellipticity ratios range from 1 to 6, and for cones whose maximum semiapex angle is less than 30°. Results given by the method are shown to agree well with experimental values.

17. Key Words (Suggested by Author(s))	18. Distribution Statement
Elliptic cones - pressure distribution Pressure distribution - elliptic cones	Unclassified - Unlimited

19. Security Classif. (of this report)	20. Security Classif. (of this page)	21. No. of Pages	22. Price*
Unclassified	Unclassified	26	$3.00

*For sale by the Clearinghouse for Federal Scientific and Technical Information
Springfield, Virginia 22151

NOTATION

A^*	relative area of a sector of an elliptical quadrant (sketch (a))
a	semiminor axis of an ellipse
b	semimajor axis of an ellipse
C_C	chord-force coefficient based on base area of elliptic cone
C_D	drag-force coefficient based on base area of elliptic cone
C_L	lift-force coefficient based on base area of elliptic cone
C_N	normal-force coefficient based on base area of elliptic cone
C_p	surface pressure coefficient
C_{p_c}	surface pressure coefficient on circular cone at zero angle of attack
C_{p_w}	surface pressure coefficient on two-dimensional wedge
$C_{p_{yo}}$	surface pressure coefficient on elliptic cone at zero angle of attack in vertical plane of symmetry
$C_{p_{y\alpha+}}$	windward surface pressure coefficient on elliptic cone at angle of attack in vertical plane of symmetry
$C_{p_{y\alpha-}}$	leeward surface pressure coefficient on elliptic cone at angle of attack in vertical plane of symmetry
$C_{p_{zo}}$	surface pressure coefficient on elliptic cone at zero angle of attack in horizontal plane of symmetry
$C_{p_{z\alpha}}$	surface pressure coefficient on elliptic cone at angle of attack in horizontal plane of symmetry
$C_{p_{\alpha+}}$	windward surface pressure coefficient on elliptic cone at angle of attack
$C_{p_{\alpha-}}$	leeward surface pressure coefficient on elliptic cone at angle of attack
d	differential operator
$k_{1,2,3}$	interpolation constants in equation (A1)
l	length of elliptic cone
M_∞	free-stream Mach number

m	slope of pressure distribution curve with respect to A^* at horizontal plane of symmetry (sketch (b))
n	exponent characterizing pressure distribution at zero angle of attack
$n+$	exponent characterizing windward incremental surface pressure distribution due to angle of attack
$n-$	exponent characterizing leeward incremental surface pressure distribution due to angle of attack
$S_{1C}(n)$	normalized value of pressure distribution integral with respect to A^* at angle of attack
$S_{1N}(n)$	normalized value of pressure distribution integral with respect to z/b at angle of attack
$S_{2C}(n)$	normalized value of pressure distribution integral with respect to A^* at zero angle of attack
$s(A^*)$	normalized pressure distribution function (eq. (4))
y	vertical coordinate
z	horizontal or spanwise coordinate
α	angle of attack
ΔC_C	incremental chord-force coefficient due to angle of attack
ΔC_{p_z}	incremental pressure on cone due to angle of attack in horizontal plane of symmetry
ΔC_α	incremental surface pressure coefficient due to angle of attack ($\alpha+$ windward surface, $\alpha-$ leeward surface)
δ_c	circular cone semiapex angle
δ_{wo}	equivalent two-dimensional wedge angle, zero angle-of-attack case
$\delta_{w\alpha}$	equivalent two-dimensional wedge angle, angle-of-attack case
δ_y	semiapex angle of elliptic cone in vertical plane of symmetry
δ_z	semiapex angle of elliptic cone in horizontal plane of symmetry
δ^*	proportionality constant (eq. (6))
μ	slope of correlation line (fig. 1)
ψ	polar coordinate (sketch (a))

A METHOD FOR PREDICTING PRESSURES ON ELLIPTIC CONES AT SUPERSONIC SPEEDS

George E. Kaattari

Ames Research Center

SUMMARY

A method is presented for estimating the pressure distribution over elliptic cones at supersonic Mach numbers and angle of attack. The method is based on an empirical correlation between experimental pressures in the symmetry planes of elliptic cones and the pressures given by two-dimensional shock theory. The method is applicable for Mach numbers greater than 2, for cones whose ellipticity ratios range from 1 to 6, and for cones whose maximum semiapex angle is less than 30°. Results given by the method are shown to agree well with experimental values.

INTRODUCTION

Studies have shown that an elliptic cone can develop reasonably high lift-drag ratios and yet provide usable volume. Such a body, equipped with suitable stabilizing surfaces, offers possibilities as a supersonic flight vehicle.

Exact theoretical solutions for pressure distributions on elliptic cones at angle of attack are difficult to derive and are usually numerical solutions to exact equations requiring machine computation. Approximate solutions for pressure distribution are given by Newtonian theory and by the tangent cone method. In many cases these approximate methods give pressure distributions that agree well with experimental values; however, there are ranges of Mach number and cone geometry in which good results are not obtained. Both methods fail to account for pressures over the leeward surface of a cone when it is shielded from the free stream by angle of attack.

This report presents a semiempirical method with which pressure distributions over the entire surface of an elliptic cone can be estimated with good accuracy for a wide range of Mach numbers, cone geometry, and angles of attack.

ANALYSIS

The analysis required for predicting pressure distributions on elliptic cones will be developed in two parts. First, the zero angle-of-attack case is considered. The analysis is based on an experimentally suggested invariance of chord-force coefficient with cone section ellipticity (ref. 1) and on a

linear correlation of experimental pressures on the symmetry planes of elliptic cones with two-dimensional values from shock theory. This information is sufficient for predicting the pressure distribution over the cone surface. Next, the analysis will be extended to the angle-of-attack case. The pressures on the symmetry planes of the cone at angle of attack will also be shown to correlate in a simple way with values from two-dimensional shock theory. These symmetry plane pressures plus additional correlations to be described in detail then provide information sufficient to estimate pressure distributions closely on a cone surface at angle of attack.

Elliptic Cones at Zero Angle of Attack

Chord force- Experimental investigation of elliptic cones (ref. 1) indicates that for a given Mach number, cone length, and base area, the chord force is constant over a large range in the ellipticity ratio, b/a, of the cone cross section at zero angle of attack. This result is predicted by slender body theory in which the chord force depends only on the maximum cross-sectional area and is independent of shape. Newtonian theory also gives this result for small ellipticity ratio or, in any case, if the maximum angle of the cone apex is less than about 30°. The assumption was accordingly made that the zero angle-of-attack chord-force coefficient of an elliptic cone at a given Mach number is equal to that of a circular cone of the same length and base area.

Correlation of conical and two-dimensional pressures- Typical correlations developed between experimental pressures (refs. 1,2) in the symmetry planes of elliptic cones and the corresponding two-dimensional or wedge pressures when the wedge angles are equal to the cone semiapex angles in the vertical, y, and horizontal, z, planes of symmetry are shown in figure 1. Linear correlations result at a given Mach number for a family of cones that have the same ratio of base area to length but differ in cross-section ellipticity. The circular cones are identified by filled symbols. The pressures at these coordinate points may be readily determined from supersonic handbooks (e.g., ref. 3). The appropriate cone for each family, fixed by the constant base area and length requirement, has the semiapex angle, δ_c, determined from

$$\tan \delta_c = \sqrt{(\tan \delta_y)(\tan \delta_z)} = \sqrt{ab}/l \qquad (1)$$

The value of the slope, $\mu = dC_p/dC_{p_w}$, would then completely define the correlation line. The pressures in the symmetry planes of any elliptic cone in the family could then be determined from the correlation line with the two-dimensional (wedge) pressure coefficient corresponding to the cone angle in the plane of symmetry and the free-stream Mach number.

Experimentally determined slopes μ (refs. 4,5) including those of figure 1 and certain theoretical values (ref. 6) were plotted on logarithmic scales as a function of the ratio of circular cone pressure to wedge pressure. The general, linear correlation shown in figure 2 was found to result for the wide range of cone geometries and Mach numbers shown. This correlation is closely represented by

$$\mu = \left(C_{p_c}/C_{p_w}\right)^{1.6} \tag{2}$$

The correlation lines of figure 1 are thus completely specified by C_{p_c}/C_{p_w} and may be constructed for any family of elliptic cones without appeal to experiment since accurate theoretical values of pressure coefficients for circular cones and two-dimensional wedges are available.

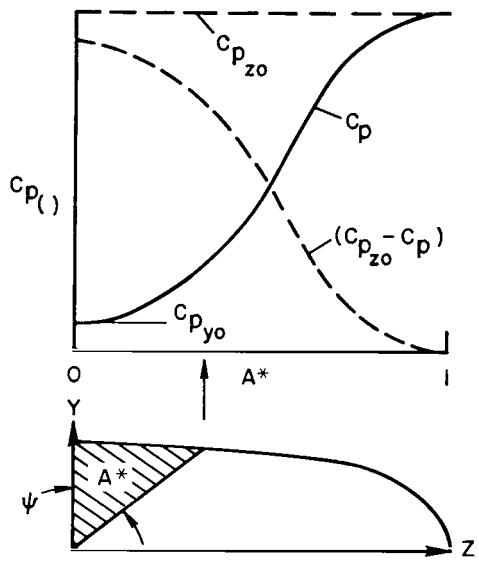

Sketch (a)

Pressure distribution- A typical pressure distribution on an elliptic cone at zero angle of attack is represented in sketch (a) by the solid curve, C_p. The dashed curves represent a decompositon of the solid curve into $C_{p_{zo}}$ and $C_{p_{zo}} - C_p$ curves. The abscissa, A*, represents the ratio of the area of the indicated sector to that of the whole quadrant. The variable A* is utilized since the integral of the pressure distribution curve, C_p, is then equal to the chord-force coefficient referred to the base area which, in view of previous discussion, is equal to the pressure coefficient, C_{p_c}, of the equivalent circular cone. Symmetry considerations require that the derivatives of the pressure distribution curves with respect to A* be zero at A* = 0 and at A* = 1.

The known pressures $C_{p_{yo}}$, $C_{p_{zo}}$, and C_{p_c} are related as follows:

$$C_{p_c} = \int_0^1 C_p \, dA^* = C_{p_{zo}} - \int_0^1 (C_{p_{zo}} - C_p)\,dA^* = C_{p_{zo}} - (C_{p_{zo}} - C_{p_{yo}}) \int_0^1 s(A^*)\, dA^*$$

or

$$\frac{C_{p_{zo}} - C_{p_c}}{C_{p_{zo}} - C_{p_{yo}}} = \int_0^1 s(A^*)dA^* = S_{2C}(n) \tag{3}$$

The term $s(A^*)$ represents the monotonically decreasing curve $(C_{p_{zo}} - C_p)$ normalized to have the value of unity (1) at A* = 0. A simple, monotonically decreasing function having the required properties $s(0) = 1$, $s(1) = 0$, $d[s(0)]/dA^* = 0$, and $d[s(1)]/dA^* = 0$ was chosen to represent $s(A^*)$

$$s(A^*) = \frac{1 + \cos \pi (A^*)^n}{2} \tag{4}$$

Values of the integral (eq. (3)) were found for various values of n. The results, represented by $S_{2C}(n)$ as a function of n, are plotted in figure 3.

Since the pressure ratio

$$\left(C_{p_{zo}} - C_{p_c}\right) \Big/ \left(C_{p_{zo}} - C_{p_{yo}}\right) = S_{2C}(n)$$

is known, the value of n corresponding to $S_{2C}(n)$ is also known from figure 3. The pressure distribution curve, C_p, as a function of A^* is then determined with equation (5).

$$C_p = \frac{C_{p_{zo}} + C_{p_{yo}}}{2} - \frac{C_{p_{zo}} - C_{p_{yo}}}{2} \cos \pi(A^*)^n \tag{5}$$

Elliptic Cones at Angle of Attack

Pressures in the vertical plane of symmetry- The method for estimating the pressures on an elliptic cone in the vertical plane of symmetry at angle of attack is as follows: The required angle, $\delta_{w\alpha}$, for a two-dimensional wedge was determined so that the associated wedge pressure would equal the experimental pressure on the cone element in the vertical plane of symmetry. A linear relationship was assumed between the required angle, $\delta_{w\alpha}$, and the total inclination $\delta_y + \alpha$ of the cone element. The proportionality constant δ^* was determined at zero angle of attack and assumed to be valid at angle of attack, that is

$$\left.\begin{aligned} \frac{\delta_{wo}}{\delta_y} = \delta^* = \frac{\delta_{w\alpha}}{\delta_y + \alpha} \\ \delta_{w\alpha} = \delta^*(\delta_y + \alpha) \end{aligned}\right\} \tag{6}$$

or

The pressure on the cone in the vertical plane of symmetry is then that of a two-dimensional wedge at the same Mach number and whose surface is inclined at the angle, $\delta_{w\alpha}$, as determined with equation (6).

Equation (6) was verified by good correlation between predicted and experimental pressures as shown in figure 4 for a variety of cones at different Mach numbers and angles of attack.

Pressures in the horizontal plane of symmetry- The method for estimating the pressure coefficient in the horizontal plane of symmetry on elliptic cones was based on an empirical modification of Newtonian theory. Newtonian theory gives the following expression for the variation of pressure in the horizontal plane of symmetry on an elliptic cone with angle of attack.

$$\left.\begin{aligned} C_{p_{z\alpha}} = C_{p_{zo}} \cos^2 \alpha \\ \frac{C_{p_{zo}} - C_{p_{z\alpha}}}{\sin^2 \alpha} = \frac{\Delta C_{p_z}}{\sin^2 \alpha} = C_{p_{zo}} \end{aligned}\right\} \tag{7}$$

or

Values for $C_{p_{z\alpha}}$ given by exact theory in reference 7 for various circular cones, angles of attack, and Mach numbers were plotted in figure 5 with the coordinates indicated by equation (7). A linear correlation of the low angle ($0° < \alpha < 5°$) data represented by solid symbols is evident. It was discovered that the ordinate, $\Delta C_{p_z}/\sin^2 \alpha$, multiplied by the term, $M_\infty \sin \delta_z$, brought into correlation the data of those cones whose "effective" slenderness parameter, $M_\infty \sin \delta_z$, was less than unity. The higher angle-of-attack data approach the lower or Newtonian correlation. This is to be expected since at angles of attack approaching 90° the pressure, $C_{p_{z\alpha}}$, will be substantially zero by any theory, that is, $\Delta C_{p_z} = C_{p_{zo}}$. An interpolation technique for estimating the effect of angle of attack between the empirical low-angle correlation curve, $\Delta C_{p_z}/\sin^2 \alpha = 0.500 + 1.33 C_{p_{zo}}$, and the high-angle correlation curve, $\Delta C_{p_z}/\sin^2 \alpha = C_{p_{zo}}$, is discussed in the appendix. The essential results of the interpolation are presented in figure 6 as $\Delta C_{p_z}/C_{p_{zo}}$ as a function of angle of attack, α, for various values of the parameter, $(0.500 + 1.33 C_{p_{zo}})/(C_{p_{zo}} M_\infty \sin \delta_z)$.

Although the above correlation was based on the data for circular cones, it is assumed to be valid for elliptic cones as well. This assumption is indirectly confirmed by good chord-force predictions for highly elliptic cones at angle of attack.

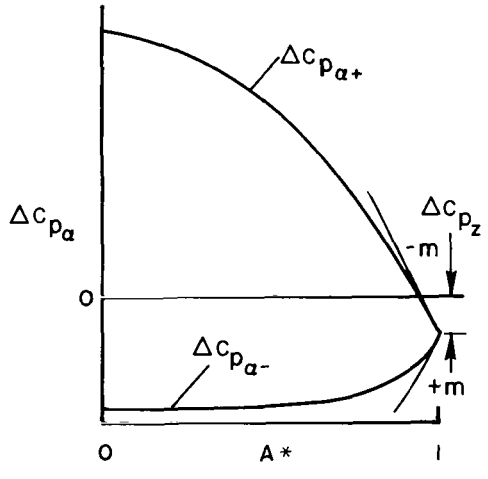

Sketch (b)

Pressure distribution- Typical incremental pressure distributions on an elliptic cone due to angle of attack are shown in sketch (b). Curves $\Delta C_{p_{\alpha+}}$ and $\Delta C_{p_{\alpha-}}$ represent the incremental pressure distributions on the windward and leeward surfaces of the cone, respectively. In this case, symmetry considerations require that the slopes of these curves in the vertical plane of symmetry ($A^* = 0$) are zero at all angles of attack. It is again assumed that these pressure distribution curves are of uniformly decreasing or increasing value over the interval $0 < A^* < 1$. The curve of $\Delta C_{p_{\alpha+}}$ has the slope -m at $A^* = 1$ and the curve of $\Delta C_{p_{\alpha-}}$ has the slope +m at $A^* = 1$. Simple monotonic functions of A^* having zero slope at $A^* = 0$ and a nonzero slope at $A^* = 1$ were used to represent the pressure distribution curves shown in sketch (b).

$$\Delta C_{p_{\alpha+}} = C_{p_{\alpha+}} - C_p = \left[\left(C_{p_{y\alpha+}} - C_{p_{yo}}\right) + \Delta C_{p_z}\right] \cos\left[(\pi/2)(A^*)^{n+}\right] - \Delta C_{p_z} \tag{8a}$$

$$\Delta C_{p_{\alpha-}} = C_{p_{\alpha-}} - C_p = -\left[\left(C_{p_{yo}} - C_{p_{y\alpha-}}\right) - \Delta C_{p_z}\right]\cos\left[(\pi/2)(A^*)^{n-}\right] - \Delta C_{p_z} \quad (8b)$$

The average value of the integrals with respect to A^* of equations (8) gives the incremental chord-force coefficient, ΔC_C, due to angle of attack as expressed in the following:

$$\Delta C_C = \frac{\left[\left(C_{p_{y\alpha+}} - C_{p_{yo}}\right) + \Delta C_{p_z}\right]S_{1C}(n+) - \left[\left(C_{p_{yo}} - C_{p_{y\alpha-}}\right) - \Delta C_{p_z}\right]S_{1C}(n-)}{2} - \Delta C_{p_z} \quad (9)$$

The functions $S_{1C}(n)$ required in equation (9) are defined by the integral

$$S_{1C}(n) = \int_0^1 \cos\left[(\pi/2)(A^*)^n\right]dA^* \quad (10)$$

A plot of $S_{1C}(n)$ as a function of n is given in figure 7.

The normal-force coefficient is the difference between pressure coefficient curves $\Delta C_{p_{\alpha+}}$ and $\Delta C_{p_{\alpha-}}$ (sketch (b)) integrated with respect to the normalized span variable, $z/b = \sin(\pi A^*/2)$. The result is

$$C_N = \frac{\left(C_{p_{y\alpha+}} - C_{p_{yo}} + \Delta C_{p_z}\right)S_{1N}(n+) + \left(C_{p_{yo}} - C_{p_{y\alpha-}} - \Delta C_{p_z}\right)S_{1N}(n-)}{\pi \tan \delta_y} \quad (11)$$

where the function $S_{1N}(n)$ is defined by the integral

$$S_{1N}(n) = \int_0^1 \cos\left[\left(\frac{\pi}{2}\right)^{1-n}\left(\sin^{-1}\frac{z}{b}\right)^n\right]d\left(\frac{z}{b}\right) \quad (12)$$

A plot of $S_{1N}(n)$ as a function of n is given in figure 7. The normal-force coefficient is determined with equation (11) when the values for n are specified.

The values for n required in equations (8), (9), and (11) are considered next. Newtonian theory gives the result for the pressure derivative m indicated in sketch (b) that

$$m = \frac{dC_p}{dA^*} = \left(2 \sin^2 \delta_z\right)\frac{\pi \sin 2\alpha}{2 \tan \delta_y} \quad (13)$$

The slope m of pressure distribution curves given by a more sophisticated (exact) theory of reference 7 for circular cones were compared with Newtonian values in figure 8. Surprisingly good agreement between Newtonian values and exact values was found as shown.

The foregoing discussions in regard to incremental pressure distribution due to angle of attack and to the pressure derivative m in the horizontal plane of symmetry apply directly to circular cones that have a uniform pressure at zero angle of attack. In the case of elliptic cones, a modification to the Newtonian pressure derivative is required. This correction takes into account the fact that an elliptic cone does not have constant zero angle-of-attack reference pressure distribution and although the pressure derivative is zero at $A^* = 1$, it rapidly assumes a value other than zero for $A^* < 1$. It was found for a wide range of cone ellipticity ratios that a good approximation to the zero angle-of-attack pressure distribution was characterized by a curve whose average pressure derivative in the vicinity of $A^* = 1$ is $2(C_{p_{zo}} - C_{p_{yo}})$ as indicated in sketch (c). Therefore, an improved slope for the incremental pressure distribution in the vicinity of $A^* = 1$ is obviously given if the slope term $2(C_{p_{zo}} - C_{p_{yo}})$ is added to the slope . m given by equation (13). The correction to m should be subtracted for the leeward pressure distribution; however, a discontinuity in pressure slope would then be imposed at $A^* = 1$. The corrective term $2(C_{p_{zo}} - C_{p_{yo}})$ was therefore applied in the positive sense to both windward and leeward pressure distribution calculations to avoid this discontinuity. The values for n+ and n- are related to this modified slope by differentiating equations (8) and recalling that $dC_p/dA^* = 0$ at $A^* = 1$.

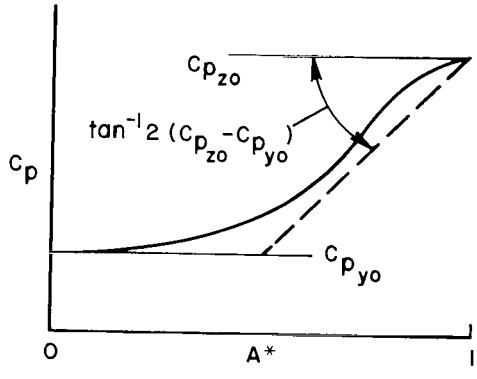

Sketch (c)

Curve $\Delta C_{p_{\alpha+}}$

$$\frac{dC_{p_{\alpha+}}}{dA^*} = -\left(C_{p_{y\alpha+}} - C_{p_{yo}} + \Delta C_{p_z}\right)\frac{\pi}{2}(n+) = -\left[m + 2\left(C_{p_{zo}} - C_{p_{yo}}\right)\right]$$

or

$$(n+) = \frac{2\left[m + 2\left(C_{p_{zo}} - C_{p_{yo}}\right)\right]}{\pi\left(C_{p_{y\alpha+}} - C_{p_{yo}} + C_{p_z}\right)} \qquad (14a)$$

Curve $\Delta C_{p_{\alpha-}}$

$$\frac{dC_{p_{\alpha-}}}{dA^*} = \left(C_{p_{yo}} - C_{p_{y\alpha-}} - \Delta C_{p_z}\right)\frac{\pi}{2}(n-) = m + 2\left(C_{p_{zo}} - C_{p_{yo}}\right) \qquad (14b)$$

or

$$(n-) = \frac{2\left[m + 2\left(C_{p_{zo}} - C_{p_{yo}}\right)\right]}{\pi\left(C_{p_{yo}} - C_{p_{y\alpha-}} - \Delta C_{p_z}\right)}$$

Equations (14) with equation (13) give numerical values for n+ and n-. Pressure coefficient distributions, chord- and normal-force coefficients can then be calculated with equations (8), (9), and (11) and the curves of figure 7.

COMPARISON BETWEEN EXPERIMENTAL AND PREDICTED RESULTS

The comparisons between experimental and predicted results presented herein are not exhaustive but are typical of a larger body of such comparisons made during the course of this investigation. Direct comparisons between the predicted results of the present method and other simple methods were limited to the zero angle-of-attack case.

Aerodynamic Coefficients

The validity of the method for determining pressure distribution was assessed indirectly by comparison of the integrated pressure coefficients in the form of the aerodynamic coefficients, C_L and C_D with experimental values from reference 1 presented in figure 9. These experimental data represent a wide range in cone ellipticity, $1 < b/a < 6$, at Mach numbers 2 and 3. The agreement between experimental and predicted values is considered good over the greater portion of the angle-of-attack range of the comparison. Discrepancies between experimental and predicted values are appreciable only in a few cases and then only when the angle of attack is greater than about 10°. This lack of good agreement at higher angles of attack is due to the effects of vortex flow in the wake. These effects are known to become significant with increasing angle of attack. The present method, based on inviscid flow, does not take into account any effects of vortex flow.

It should be noted that a small experimentally determined skin-friction chord-force coefficient has been taken into account in calculating the predicted values presented in figure 9 in order to make an equitable comparison.

Pressure Distributions

Zero angle of attack- Experimental and predicted pressure distributions are presented for elliptic cones at zero angle of attack in figure 10. The predicted values include those of the tangent cone method and Newtonian theory as well as those of the present method. These pressure distributions indicate that the present method gives significantly better agreement with experimental values than do the other methods for cones of ellipticity ratio, b/a = 3 and higher. For lower ellipticity ratios, the pressure distributions given by the present method are as good or better than values given by the tangent cone method. The Newtonian theory values are consistently low.

Angle of attack- Experimental and predicted pressure distributions of two elliptic cones at angle of attack and at two Mach numbers are presented in figure 11. Predicted results of the other methods considered at zero angle of attack are omitted for sake of figure clarity. The agreement between experimental and predicted pressure distributions is considered satisfactory, particularly at the higher Mach number of 6. A notable area of disagreement between predicted and experimental pressures exists at the higher angle of attack ($\alpha = 20°$) on the leeward surfaces of both cones at Mach number 3.09. This disagreement is due to the effects of vortex flow in the wake previously mentioned.

CONCLUDING REMARKS

An empirical method has been developed for predicting pressure distributions over elliptic cones at angle of attack. The method is applicable for Mach numbers above 2, for cones whose ellipticity ratio, b/a, ranges from 1 to 6, and for cones whose maximum semiapex angle does not exceed about 30°.

The method is based, primarily, on an empirical correlation between experimental pressures on the symmetry planes of elliptic cones with two-dimensional values from shock theory; and, secondarily, on correlations of spanwise pressure derivatives with parameters suggested by Newtonian theory.

Predicted pressure distributions and aerodynamic coefficients were compared with experimental values for air flows in the Mach number range from 2 to 6, with cones of ellipticity ratio, b/a, ranging from 1 to 6, and angles of attack ranging from 0° to 20°. Satisfactory agreement between predicted and experimental values was found. The predictions given by the present method are generally in better agreement with experimental values than those given by the tangent cone method or by Newtonian theory.

Ames Research Center
National Aeronautics and Space Administration
Moffett Field, Calif., 94035, May 13, 1970

APPENDIX A

DERIVATION OF THE INTERPOLATION FUNCTION USED IN PREPARING THE CURVES OF FIGURE 6

As stated previously, it was found that the change in the pressure coefficient in the horizontal plane of symmetry at low angles of attack was expressed as $\Delta C_{p_z}/C_{p_{zo}} = [(0.500 + 1.33C_{p_{zo}})/C_{p_{zo}}]\sin^2 \alpha$ and at angles of attack near 90° as $\Delta C_{p_z}/C_{p_{zo}} = \sin^2 \alpha$. In sketch (d) the slope of the line 0-1 is $(0.500 + 1.33C_{p_{zo}})/C_{p_{zo}}$, representing the low-angle correlation curve. The slope of line 0-2 is 1, and represents the Newtonian and/or high-angle-of-attack correlation curve. The solid curve represents a monotonic interpolation function of $\sin^2 \alpha$ which is tangent to the low- and high-angle correlation curves in the neighborhoods of their respective validity ($\sin^2 \alpha = 0$ and 1.0).

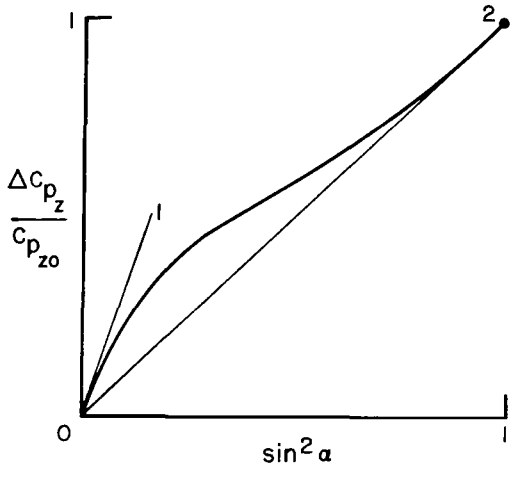

Sketch (d)

The simplest monotonic interpolation function was found to be a series expression of three terms using the ordinate, $\Delta C_{p_z}/C_{p_{zo}}$, as the independent variable; that is,

$$\sin^2 \alpha = k_1 \left(\frac{\Delta C_{p_z}}{C_{p_{zo}}}\right) + k_2 \left(\frac{\Delta C_{p_z}}{C_{p_{zo}}}\right)^2 + k_3 \left(\frac{\Delta C_{p_z}}{C_{p_{zo}}}\right)^3 \qquad \text{(A1)}$$

In order to satisfy the known slopes and ordinates required of the interpolation function, the values of the coefficients, k, were found to be

$$k_1 = \frac{C_{p_{zo}} M_\infty \sin \delta_z}{0.500 + 1.33C_{p_{zo}}}, \quad k_2 = -2(k_1 - 1), \quad \text{and} \quad k_3 = (k_1 - 1) \qquad \text{(A2)}$$

Equation (A1) was evaluated for various numerical values for k for tabulating $\sin^2 \alpha$ as a function of $(\Delta C_{p_z}/C_{p_{zo}})$. This tabulation was used to construct curves of $\Delta C_{p_z}/C_{p_{zo}}$ as a function of angle of attack, α, for various values of the parameter, k_1.

REFERENCES

1. Jorgensen, Leland H.: Elliptic Cones Alone and With Wings at Supersonic Speeds. NACA Rep. 1376, 1958.

2. Zakkay, Victor; and Visich, Marian, Jr.: Experimental Pressure Distributions on Conical Elliptical Bodies at M_∞ = 3.09 and 6.0. Pibal Rep. No. 467, AFOSR TN 59-10, AD 208 591, March 1959.

3. Ames Research Staff: Equations, Tables, and Charts for Compressible Flow. NACA Rep. 1135, 1953.

4. Chapkis, Robert L.: Hypersonic Flow Over an Elliptic Cone: Theory and Experiment. Guggenheim Aeronautical Laboratory, California Institute of Technology. Hypersonic Research Project, Memorandum No. 49, May 1, 1959.

5. Ortloff, Charles R.: Hypersonic Approximation for the Inviscid Flow Over Conical Bodies With Axial Symmetry and Comparison With Tests at Mach 8. Pibal Rep. No. 728, AFOSR 1634, Jan. 1961.

6. Van Dyke, Milton D.: The Slender Elliptic Cone as a Model for Nonlinear Supersonic Flow Theory. J. Fluid Mech., vol. 1, no. 1, May 1956, pp. 1-15.

7. Babenko, K. I.; Voskresenskiy, G. P.; Lyubimov, A. N.; and Rusanov, V. V.: Three-Dimensional Flow of Ideal Gas Past Smooth Bodies. NASA TT-F-380, 1966, from Prostranstvennoye Obtekaniye Gladkikh tel Ideal'nym Gazom Izdatel'stvo Nauka, Moscow, 1964.

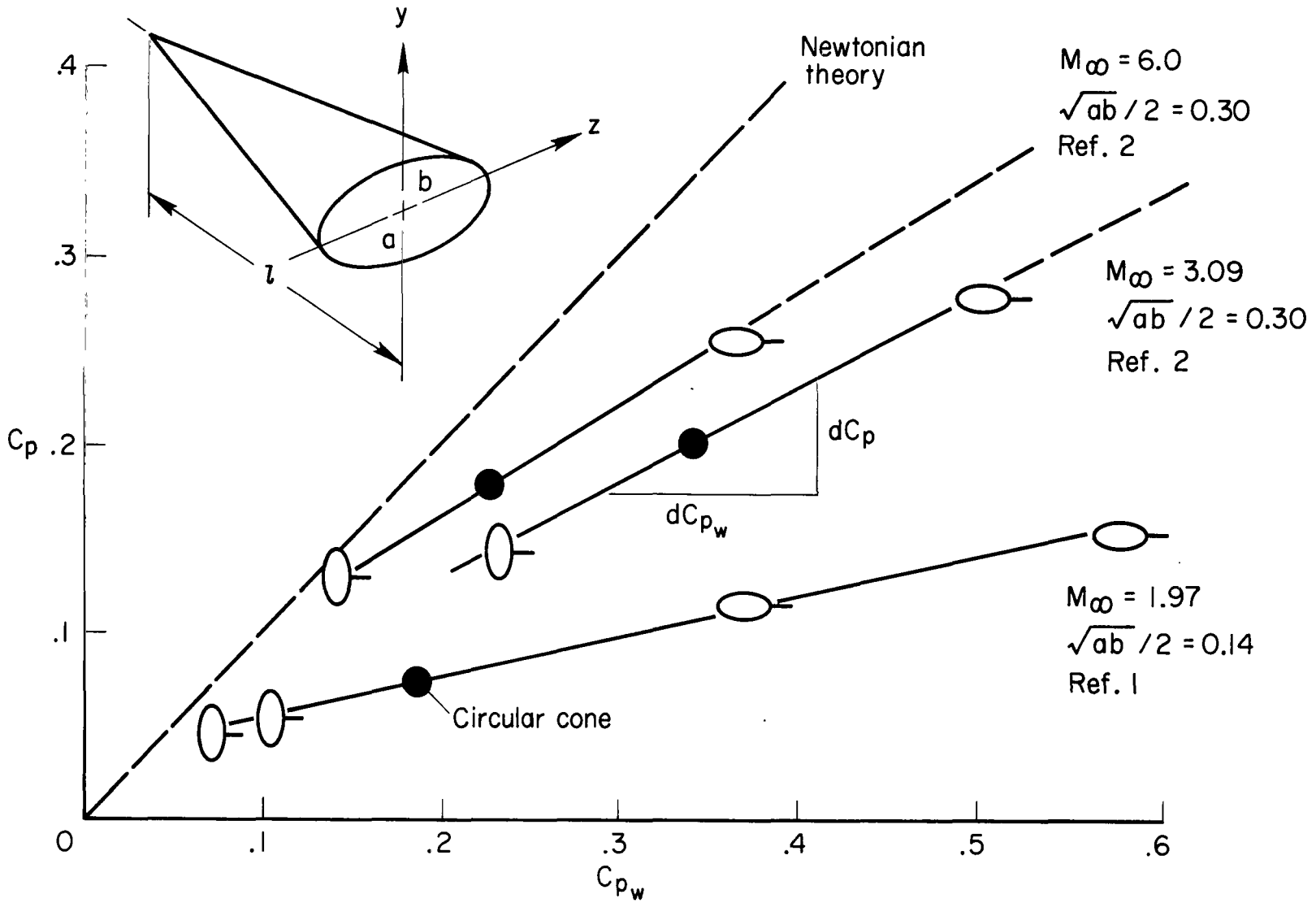

Figure 1.- Correlation of cone and wedge pressure coefficients.

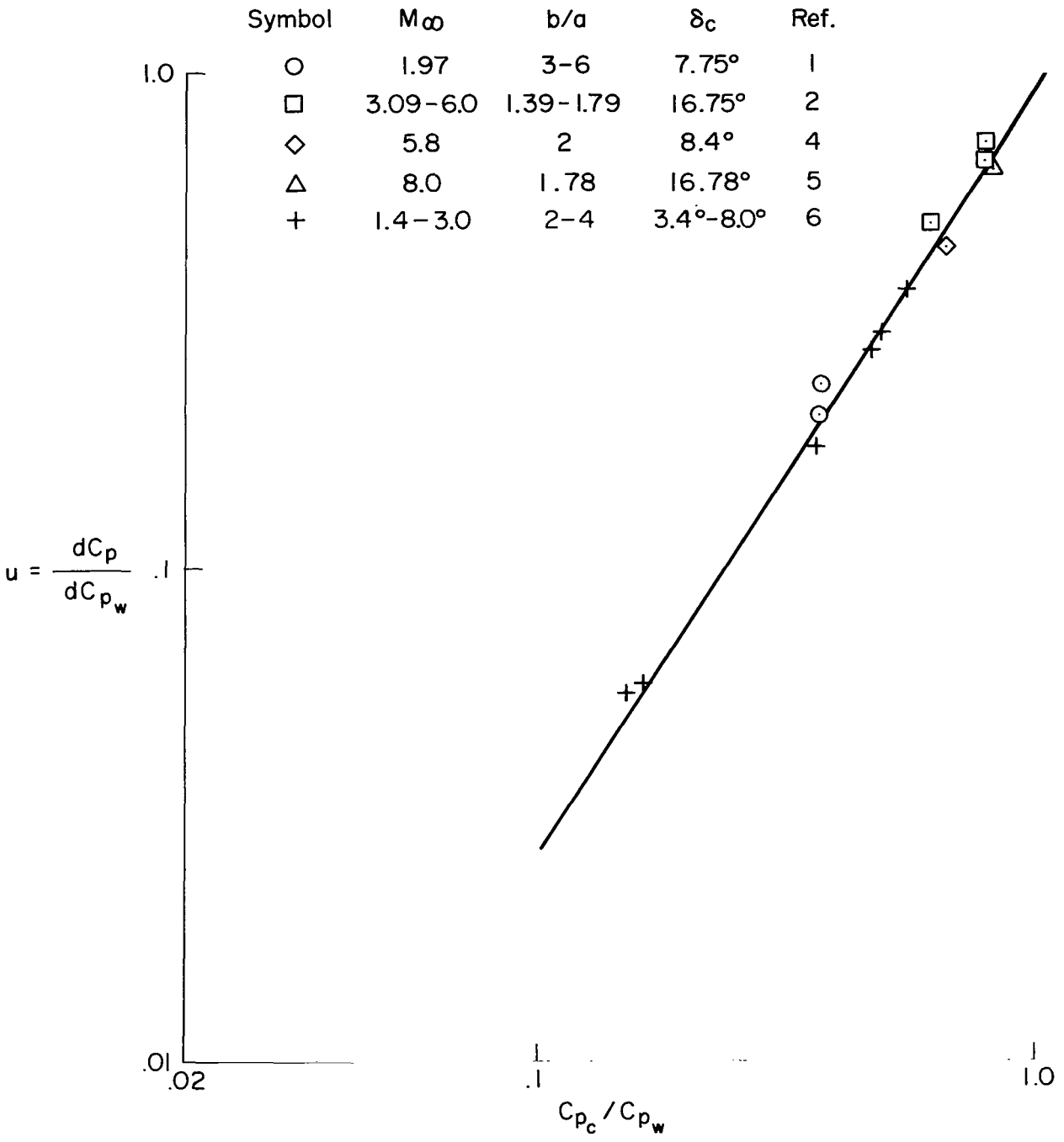

Figure 2.- Slopes of cone-wedge pressure correlation lines.

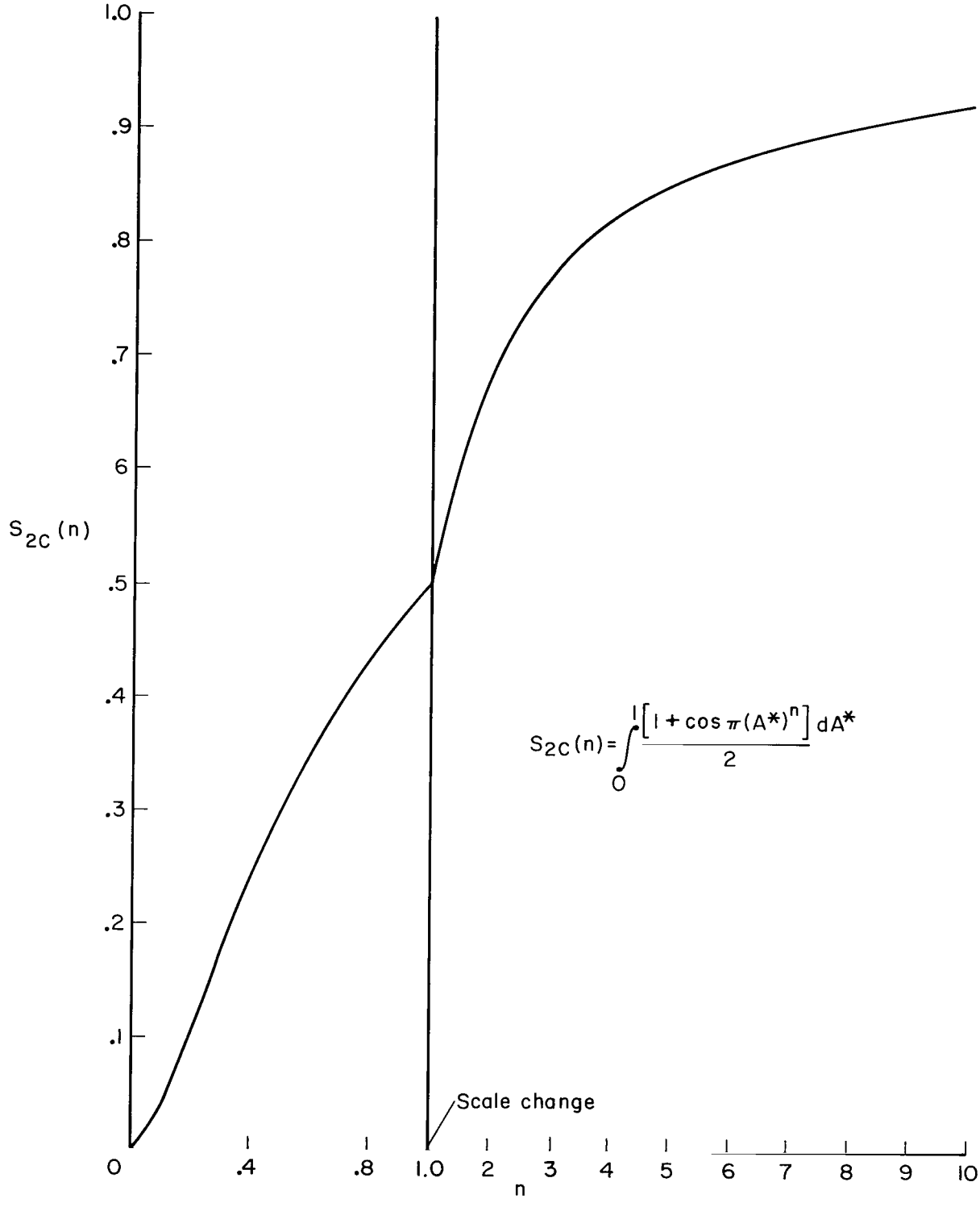

Figure 3.- The function $S_{2C}(n)$.

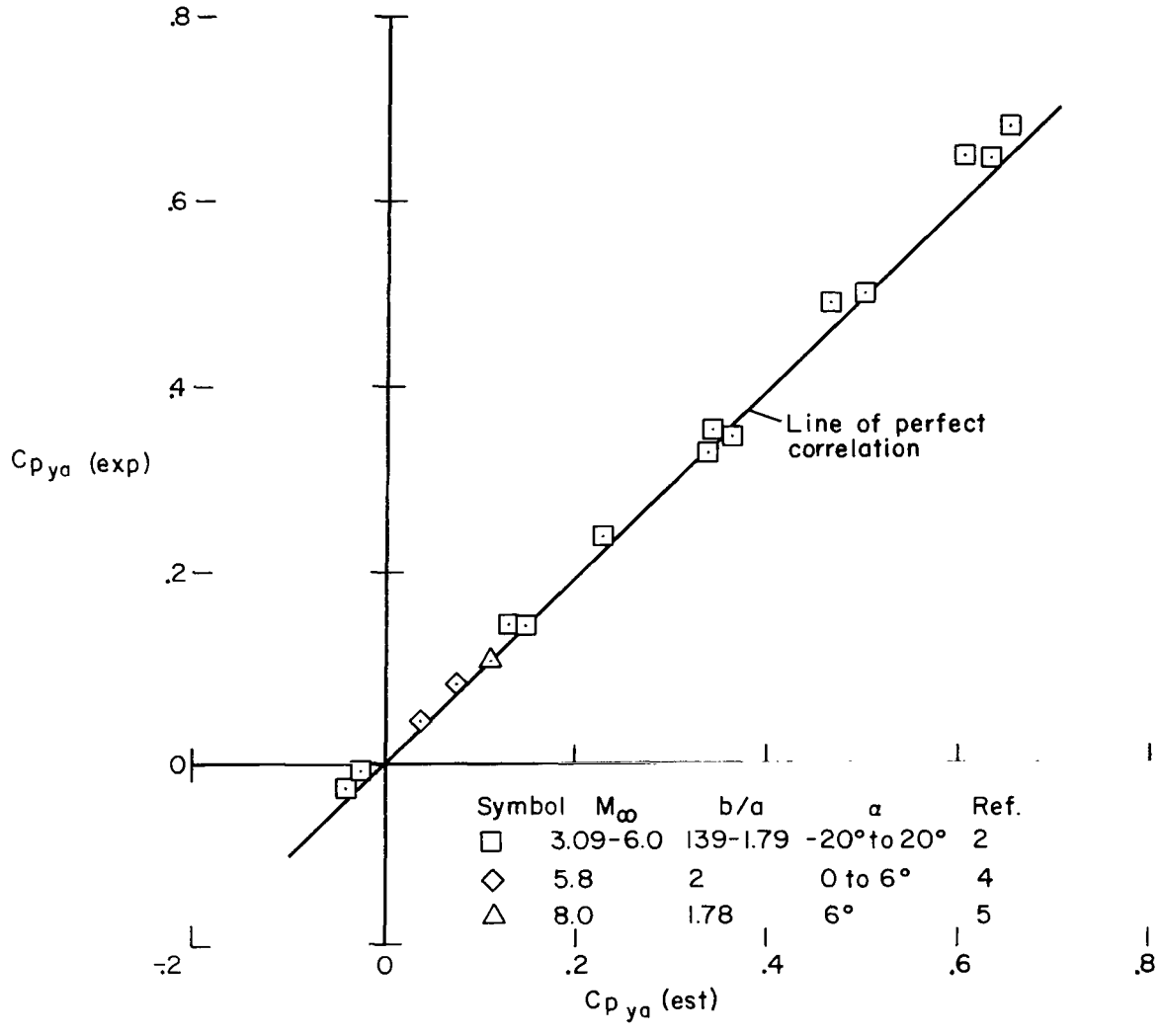

Figure 4.- Experimental and estimated pressures in the vertical plane of symmetry of elliptic cones at angle of attack.

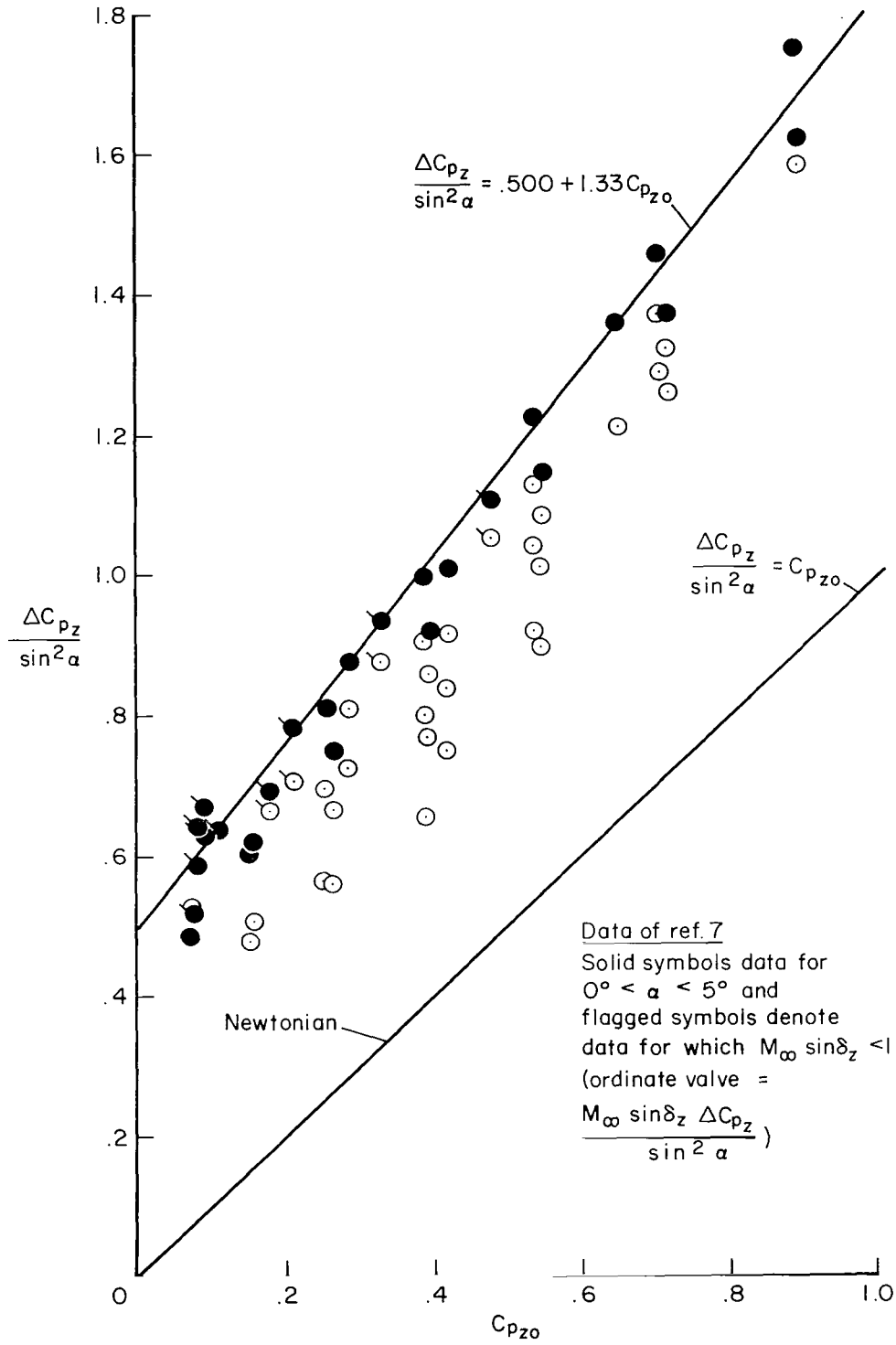

Figure 5.- Effect of angle of attack on the pressure coefficient in the horizontal plane of symmetry of cones.

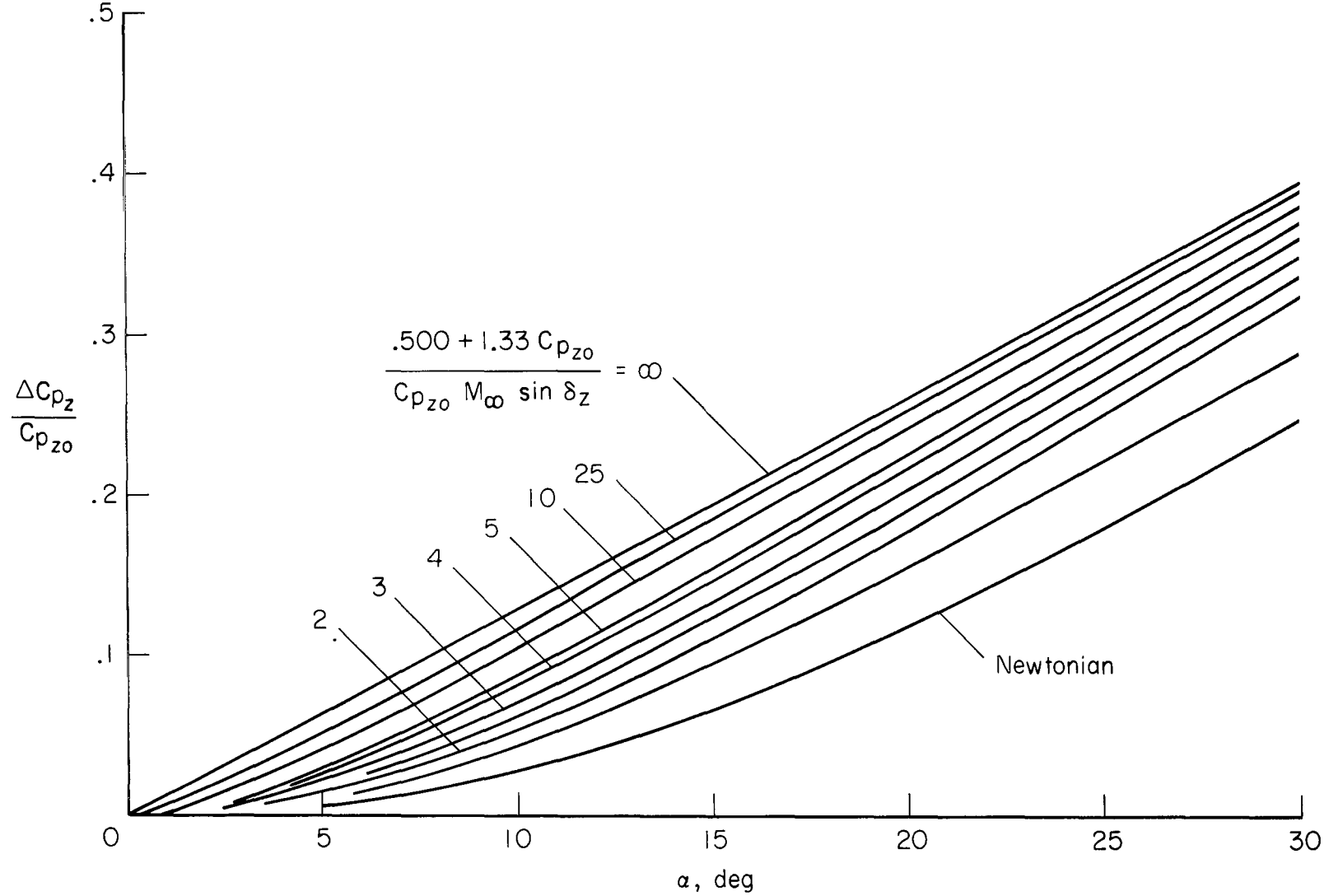

Figure 6.- Effect of angle of attack on pressure coefficient in the horizontal plane of symmetry of cones.

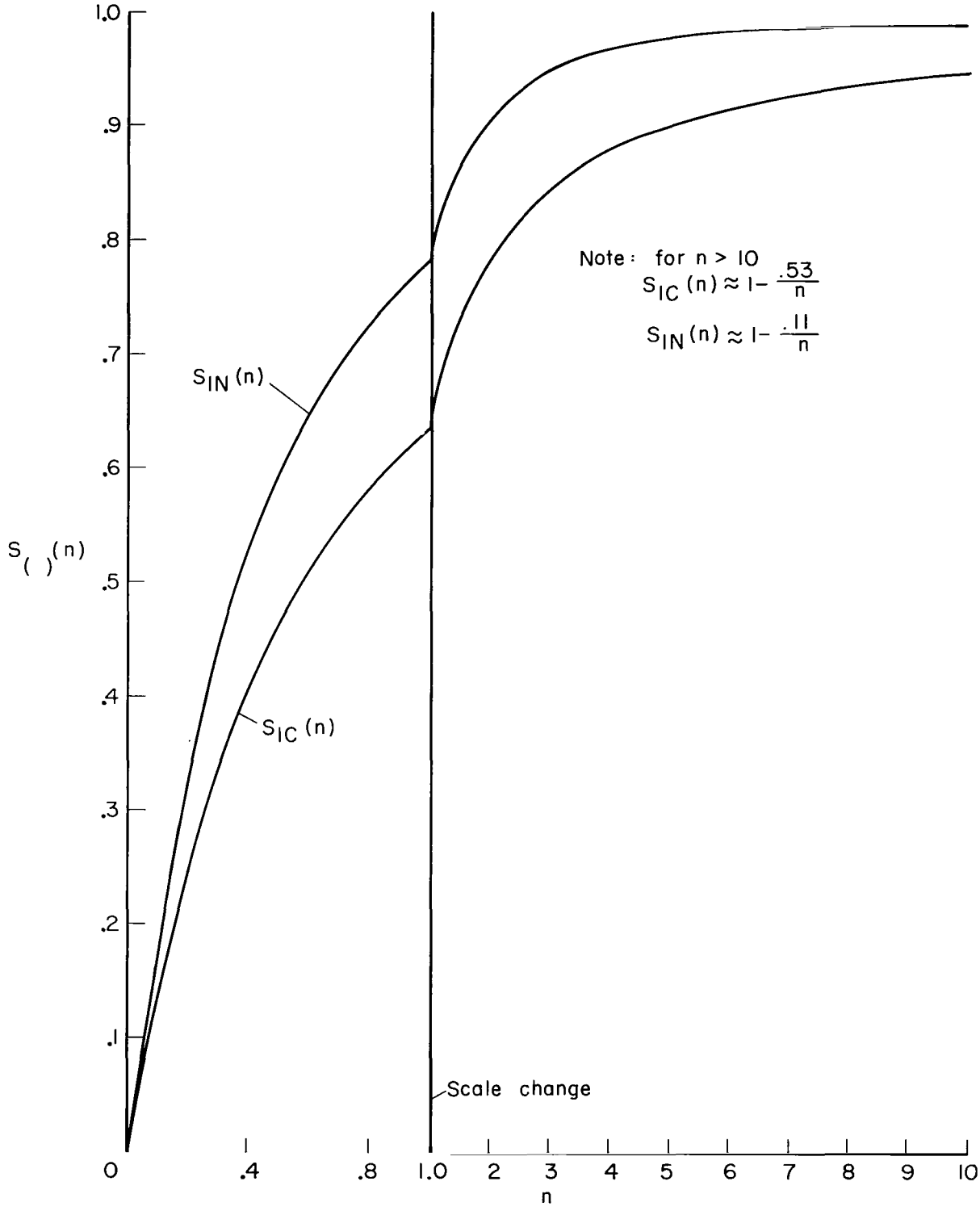

Figure 7.- The functions $S_{1C}(n)$ and $S_{1N}(n)$.

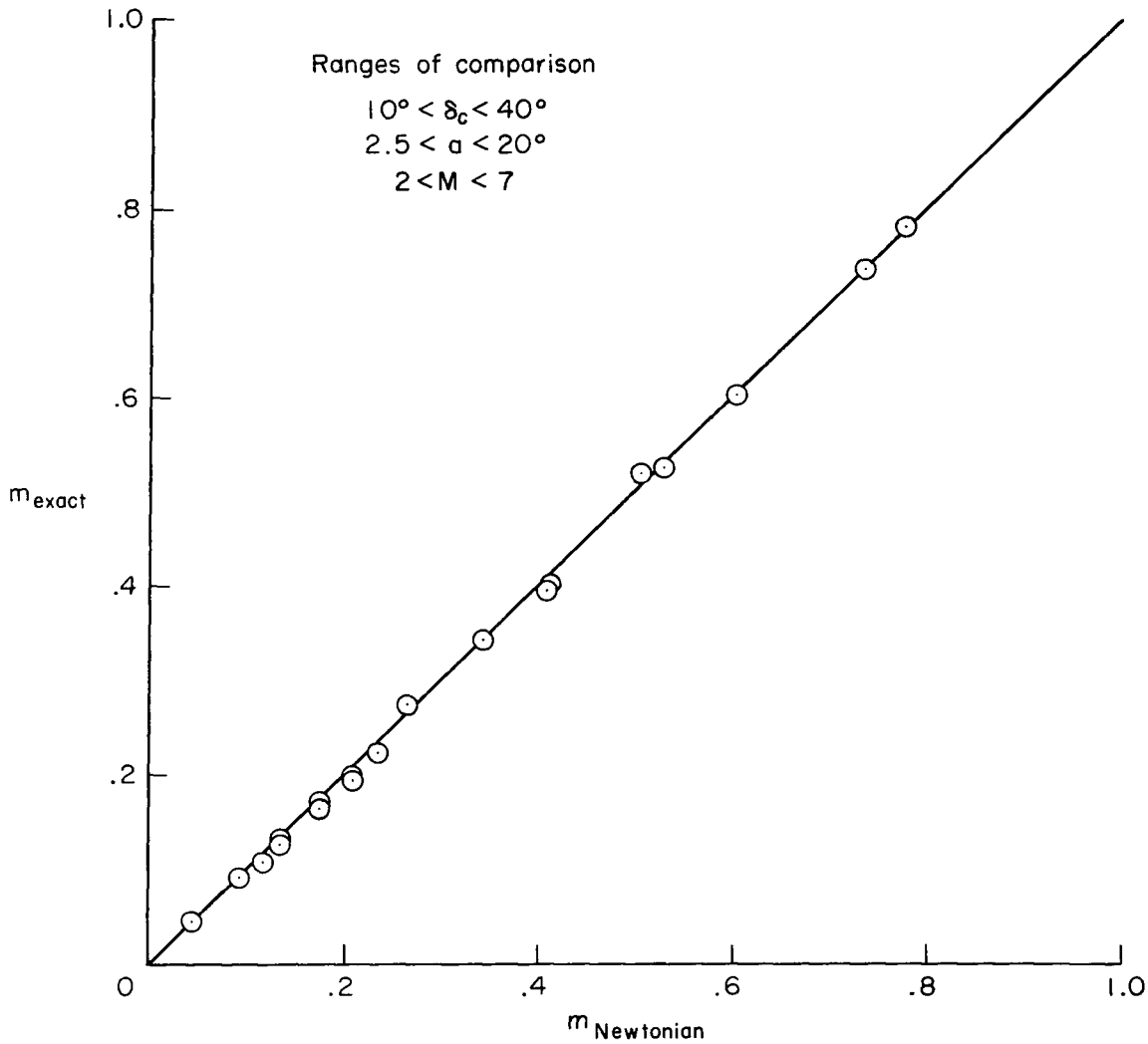

Figure 8.- Correlation of exact theory (ref. 7) and Newtonian pressure coefficient derivatives, m, in the horizontal plane of symmetry of circular cones.

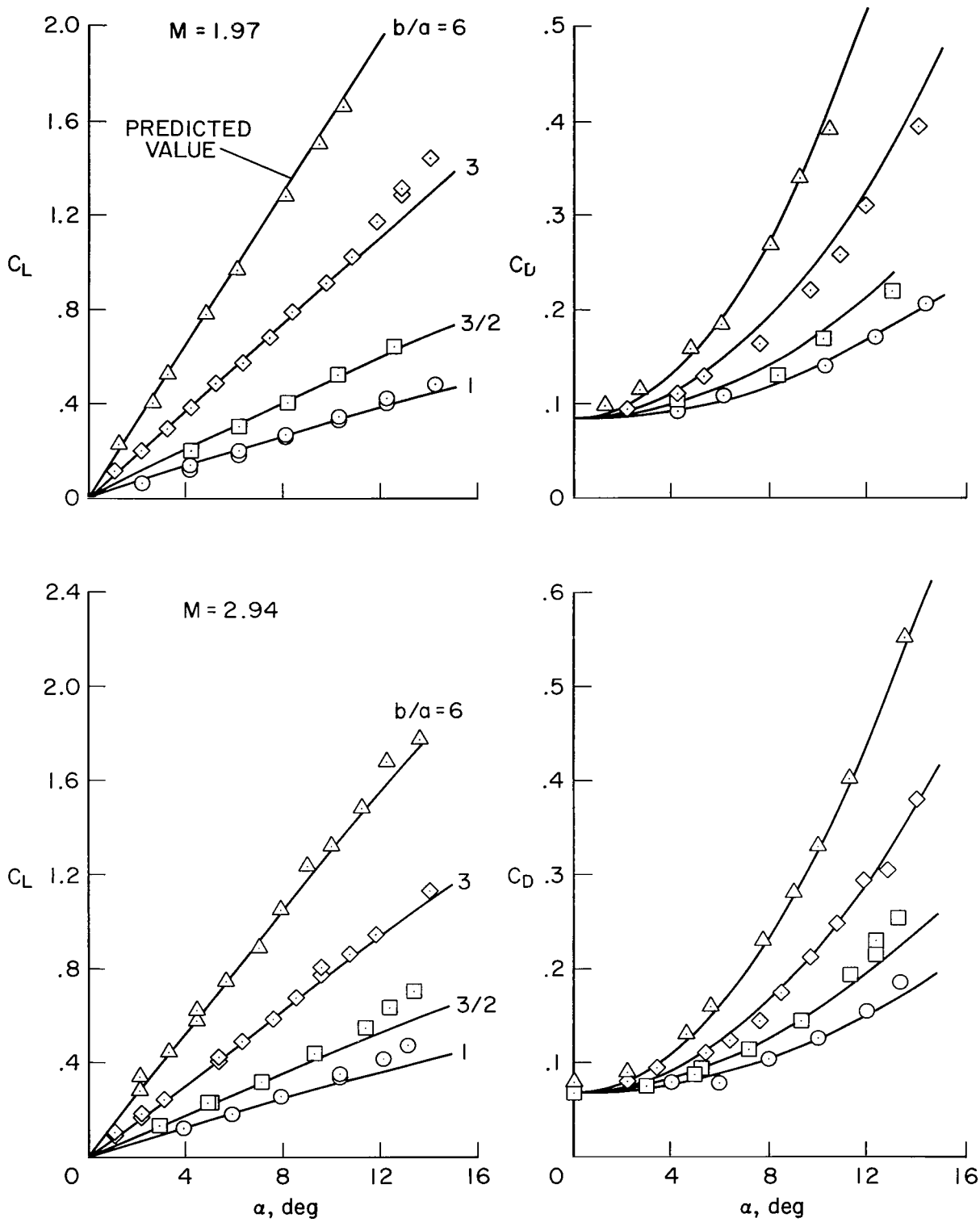

Figure 9.- Experimental and predicted aerodynamic coefficients of elliptic cones of reference 1.

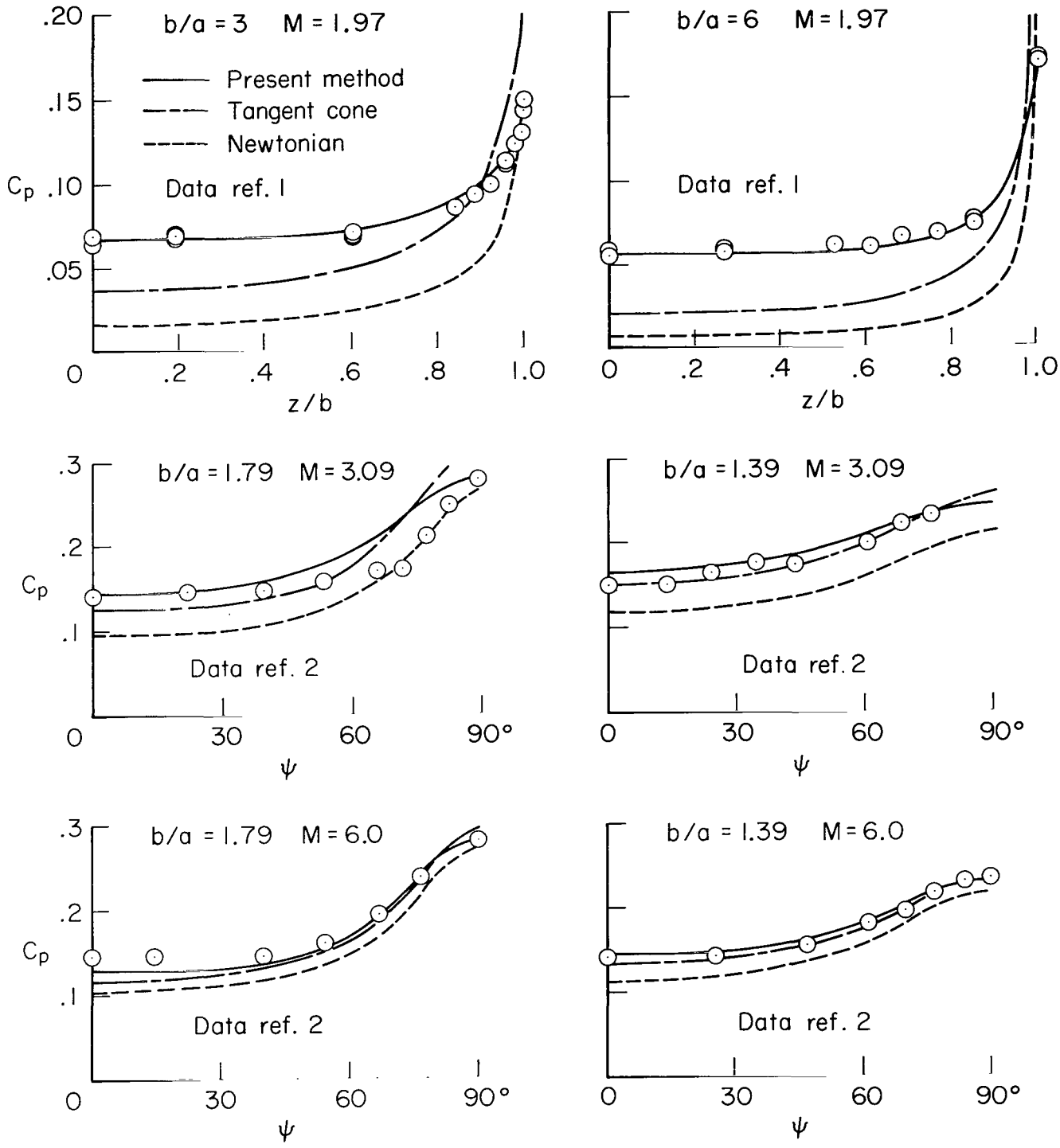

Figure 10.- Experimental and predicted pressure distributions of elliptic cones at zero angle of attack.

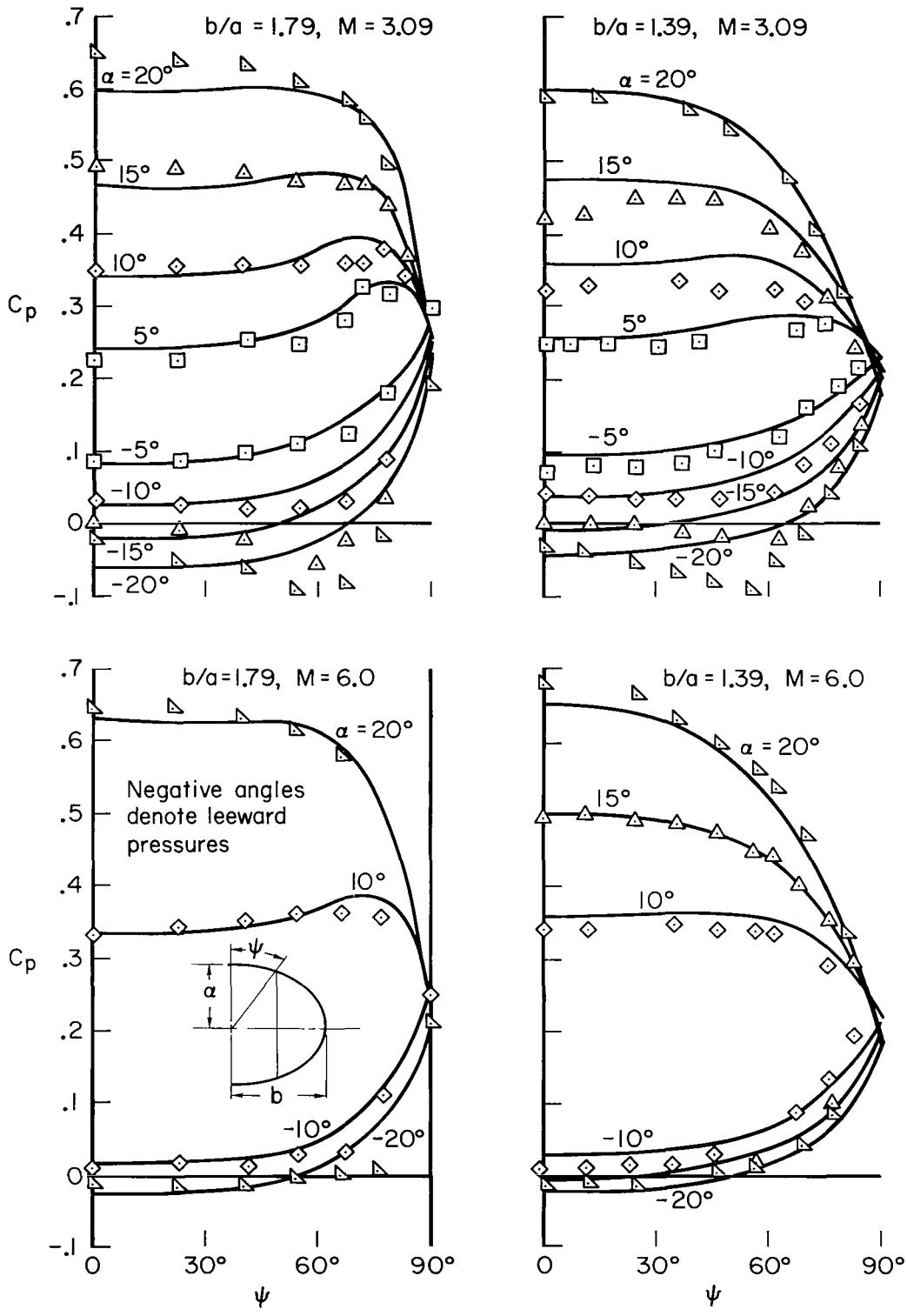

Figure 11.- Experimental and predicted pressure distributions of elliptic cones of reference 2 at angle of attack.

"The aeronautical and space activities of the United States shall be conducted so as to contribute . . . to the expansion of human knowledge of phenomena in the atmosphere and space. The Administration shall provide for the widest practicable and appropriate dissemination of information concerning its activities and the results thereof."

—NATIONAL AERONAUTICS AND SPACE ACT OF 1958

NASA SCIENTIFIC AND TECHNICAL PUBLICATIONS

TECHNICAL REPORTS: Scientific and technical information considered important, complete, and a lasting contribution to existing knowledge.

TECHNICAL NOTES: Information less broad in scope but nevertheless of importance as a contribution to existing knowledge.

TECHNICAL MEMORANDUMS: Information receiving limited distribution because of preliminary data, security classification, or other reasons.

CONTRACTOR REPORTS: Scientific and technical information generated under a NASA contract or grant and considered an important contribution to existing knowledge.

TECHNICAL TRANSLATIONS: Information published in a foreign language considered to merit NASA distribution in English.

SPECIAL PUBLICATIONS: Information derived from or of value to NASA activities. Publications include conference proceedings, monographs, data compilations, handbooks, sourcebooks, and special bibliographies.

TECHNOLOGY UTILIZATION PUBLICATIONS: Information on technology used by NASA that may be of particular interest in commercial and other non-aerospace applications. Publications include Tech Briefs, Technology Utilization Reports and Notes, and Technology Surveys.

Details on the availability of these publications may be obtained from:

SCIENTIFIC AND TECHNICAL INFORMATION DIVISION

NATIONAL AERONAUTICS AND SPACE ADMINISTRATION

Washington, D.C. 20546